

# Impregnated carbon as a susceptor material for low loss oxides in dielectric heating

B. VOS, J. MOSMAN, Y. ZHANG, E. POELS, A. BLIEK\*

*Department of Chemical Engineering, University of Amsterdam, Nieuwe Achtergracht 166, 1018 WV Amsterdam, The Netherlands*

*E-mail: blik@science.uva.nl*

Dielectric heating of materials may have distinct advantages over conventional heating in view of the fact that it is a bulk heating technique, and does not rely on conduction or convection, the driving force of which are temperature gradients. Dielectric heating is currently predominantly practised in food and ceramic processing. Research is conducted also in the areas of chemistry and in solid catalysed reactions. Base materials used in these applications, like food containers, catalysts and green ceramic products, may not demonstrate sufficiently high dielectric loss factors to allow dielectric heating to be feasible. In such cases microwave susceptor materials may be added. A whole variety of such susceptor materials are known, such as zirconia, silicon carbide and carbon. In this work, the impregnation with carbon was investigated as a way to enhance the dielectric loss factor for low loss porous oxidic materials. To this end a variety of porous oxides was impregnated with poly furfuryl alcohol which was subsequently carbonised. Impregnation conditions, dielectric heating behaviour, calculations on dielectric properties and oxidation resistance will be reported. © 2003 Kluwer Academic Publishers

## 1. Introduction

The systematic modification of low loss materials with dopants in order to increase the dielectric loss tangent and thereby to allow heating in a dielectric field is common practice, for instance to produce high loss ceramic food containers. To this end a variety of so-called susceptor materials are employed including zirconia [1, 2], silicon carbide [3] and carbon [4–6].

Susceptor materials are preferably well dispersed within the matrix of a low loss base material, in order to create a large interfacial heat transfer area and to prevent local overheating and even temperature run-aways. Silicon carbide is chemically inert to most gases and fluids and has a very high dielectric loss tangent. For this reason it is a favourable susceptor material. Alumina-SiC composites can be synthesised using a sol-gel technique [7, 8]. In this way SiC particles are covered with boehmite by deposition precipitation using aluminium nitrate and ammonia. No reports however have been published on the coating of SiC particles with other oxidic materials. Coating oxidic materials with SiC is even more difficult because the synthesis of silicon carbide involves heat treatment at elevated temperature [9–11]. Such a heat treatment could alter the structure of the oxide.

An alternative to the use of silicon carbide is amorphous carbon, which is cheap and easily prepared. Carbon itself is a high loss material [12, 13], that can be readily heated in a 2.45 GHz electromagnetic field to

temperatures in excess of 1000°C [14, 15]. Applications profiting from the ease with which carbon can be heated in a dielectric field are found in minerals processing [16, 17], desulfurisation of coal [18, 19], regeneration of carbon [20, 21], modification of carbon surface properties [22, 23], pyrolysis of coal [24, 25], synthesis of inorganic compounds and microwave induced chemical reactions [26, 27]. For composite materials of carbon black in epoxy resin it has been shown that the dielectric properties increase with volume concentration of the carbon [28, 29].

Vissers *et al.* [30] prepared carbon covered Al<sub>2</sub>O<sub>3</sub> carrier materials using pyrolysis of cyclohexane or ethane on the surface of  $\gamma$ -Al<sub>2</sub>O<sub>3</sub>. Alternatively, carbon-coating of oxidic supports may be carried out by using a carbon precursor based on coal tar pitch [31], impregnation with a polymer [32–35] or chemical vapor deposition of hydrocarbons [36]. The coating of a monolithic catalyst with carbon using a polymeric material based on furfuryl alcohol was described [37, 38]. After carbonisation at 550°C a carbon coating may be formed. Coatings with a carbon content of up to 20 wt% can be obtained.

Low loss oxides such as SiO<sub>2</sub> or Al<sub>2</sub>O<sub>3</sub> are frequently used for ceramics and catalyst supports. In the present work, we have assessed the feasibility of increasing the dielectric properties of these low oxides through impregnation with carbon as a susceptor material. We have tested the use of carbon impregnation using

\*Author to whom all correspondence should be addressed.

furfuryl alcohol polymerisation and carbonisation. The carbon content of these samples was systematically varied by changing the polymerisation conditions. Dielectric heating of both the pure and carbon impregnated oxides was tested in a 1 kW monomode cavity operated in the TE<sub>10</sub> mode at 2.45 GHz. The dielectric loss factor of the carbon-coated oxides as a function of carbon content was measured and compared to calculations based on the Rayleigh mixture equation. The resistance of the carbon layer towards oxidation was also studied.

## 2. Theory

For the solid material to be heated the dielectric energy needs to be converted into heat. The interaction of a material with a dielectric field is governed by its dimensionless complex permittivity  $\varepsilon$ :

$$\varepsilon = \varepsilon' - j \cdot \varepsilon'' \quad (1)$$

The dielectric constant  $\varepsilon'$  is a measure of the amount of energy which can be stored in a material in the form of an electrical field. The dielectric loss factor  $\varepsilon''$  is a measure of how much energy a material may dissipate in the form of heat. The dielectric loss factor is material, temperature and frequency dependent.

The dielectric properties of a material consisting of different components, such as air-solid mixtures, can be calculated from the properties of the separate components using dielectric mixture equations. Well known mixture equations are the Complex Refractive Index mixture equation, the Landau and Lifshitz, Looyenga equation, the Böttcher equation, the Bruggeman-Hani equation, the Lichtenecker equation, and the Rayleigh equation [39, 40]. The Rayleigh mixture formula describes a two component material in which material 2, consisting of small spherical particles, is dispersed in material 1:

$$\varepsilon_{\text{eff}} = \frac{\varepsilon_1(2\varepsilon_1 + \varepsilon_2) + 2\varepsilon_1\Phi(\varepsilon_2 - \varepsilon_1)}{2\varepsilon_1 + \varepsilon_2 - \Phi(\varepsilon_2 - \varepsilon_1)} \quad (2)$$

in which:  $\varepsilon_{\text{eff}}$  = complex permittivity of the mixture (-).  $\varepsilon_1$  = complex permittivity of the continuum material 1 (-).  $\varepsilon_2$  = complex permittivity of the dispersed material 2 (-).  $\Phi$  = volume fraction of material 2 in 1 (-).

The Rayleigh equation is not valid when the dispersed phase becomes a continuous phase. This is typically the case when the volume fraction of material 2 in 1 exceeds 30%. Above this volume fraction a significant statistical probability exists of finding a pathway that electrically connects two or more of the small spherical inclusions.

## 3. Experimental procedure

### 3.1. Sample preparation

#### 3.1.1. Polymerisation

Carbon coating of silica and alumina was investigated using furfuryl alcohol polymerisation and subsequent carbonisation (Table I). Silicon and aluminium oxides were dried at 150°C overnight and subsequently thoroughly mixed with furfuryl alcohol (Aldrich, 98%) in a vigorously stirred reaction vessel. Nitric acid (Acros, p.a.) was added drop wise to the suspension in order to start the polymerisation. The reaction vessel was water-

TABLE I Oxides and amount of chemicals used

Oxide	Total amount		Sample
	Furfuryl alcohol (mol · g <sub>oxide</sub> <sup>-1</sup> )	HNO <sub>3</sub> (mol · g <sub>oxide</sub> <sup>-1</sup> )	
$\gamma$ -Al <sub>2</sub> O <sub>3</sub> (trilob shaped extrudates; length × diameter = 5 × 10 <sup>-3</sup> × 2 × 10 <sup>-3</sup> m)	2.3 × 10 <sup>-2</sup>	0	A0
		1.2 × 10 <sup>-3</sup>	A1
		2.4 × 10 <sup>-3</sup>	A2
		3.6 × 10 <sup>-3</sup>	A3
		4.8 × 10 <sup>-3</sup>	A4
$\gamma$ -Al <sub>2</sub> O <sub>3</sub> (sieve fraction: d ≤ 200 μm)	2.3 × 10 <sup>-2</sup>	6.0 × 10 <sup>-3</sup>	A5
		0	B0
		1.2 × 10 <sup>-3</sup>	B1
		2.4 × 10 <sup>-3</sup>	B2
		3.6 × 10 <sup>-3</sup>	B3
SiO <sub>2</sub>	4.6 × 10 <sup>-2</sup>	0	C0
		2.4 × 10 <sup>-3</sup>	C2
		4.8 × 10 <sup>-3</sup>	C4
		7.2 × 10 <sup>-3</sup>	C6
		9.6 × 10 <sup>-3</sup>	C8
		1.2 × 10 <sup>-2</sup>	C10

TABLE II Oxides and amount of chemicals used

Oxide	Total amount			Sample
	Furfuryl alcohol (cm <sup>3</sup> )	HNO <sub>3</sub> (cm <sup>3</sup> )	Drying time (days)	
$\gamma$ -Al <sub>2</sub> O <sub>3</sub> (cylinder shaped extrudates)	2.3 × 10 <sup>-2</sup>	0	2	AC000
		1.2 × 10 <sup>-3</sup>	2	AC050
		2.4 × 10 <sup>-3</sup>	2	AC100
		4.2 × 10 <sup>-3</sup>	2	AC175
$\gamma$ -Al <sub>2</sub> O <sub>3</sub> (sieve fraction: d ≤ 200 μm)	2.3 × 10 <sup>-2</sup>	0	4	BC0
		2.1 × 10 <sup>-3</sup>	4	BC9
SiO <sub>2</sub>	4.6 × 10 <sup>-2</sup>	0	3	CC0
		4.3 × 10 <sup>-3</sup>	3	CC18
		6.4 × 10 <sup>-3</sup>	3	CC27

cooled. The addition of nitric acid was controlled in such a way to keep the temperature of the suspension at 40°C–50°C. Samples were dried overnight at 50°C in air.

#### 3.1.2. Carbonisation

Larger quantities of material (Table II) were coated with polymer, as described above. However, prolonged drying times were used. The dried material was carbonised in a fixed bed in a flow of Ar (SV = space velocity = 4 × 10<sup>-5</sup> m<sup>3</sup> s<sup>-1</sup> · kg<sup>-1</sup>). The carbonisation temperature was first raised to 150°C at a heating rate of 5°C per minute and maintained there for an hour. Subsequently the temperature was raised to 550°C at the same heating rate and maintained at that temperature for 12 hours.

#### 3.1.3. Reference material

Norit RX3 Extra is an acid washed steam activated, extruded peat-based carbon and was used as a reference material. Analysis data from the supplier are in Table III.

## 3.2. Characterisation

### 3.2.1. Pure oxides

The specific surface area and pore volume of the pure oxides was determined with N<sub>2</sub>-physisorption in a Sorptomatic 1990 (CE Instruments) (Table IV). The

TABLE III Typical analysis of Norit RX3 extra

Ash content	3 w/w%
Apparent density	400 kg · m <sup>-3</sup>
Sa	1542 m <sup>2</sup> · g <sup>-1</sup> (N <sub>2</sub> , BET)
Vp	0.77 cm <sup>3</sup> · g <sup>-1</sup> (N <sub>2</sub> )
	0.15 cm <sup>3</sup> · g <sup>-1</sup> (meso 2–50 nm)
	0.45 cm <sup>3</sup> · g <sup>-1</sup> (macro > 50 nm)

average pore width was measured using mercury intrusion in a Pascal 440 (CE Instruments). Helium density was measured using a Multi-volume 1305 pycnometer from Micromeritics.

### 3.2.2. Temperature programmed desorption (TPD)

About 70 mg of sample was placed into a porous basket in a Setaram TG85 thermo-balance and heated in Ar ( $SV = 2 \times 10^{-2} \text{ m}^3 \cdot \text{s}^{-1} \cdot \text{kg}^{-1}$ ) at a heating rate of  $10 \text{ K} \cdot \text{min}^{-1}$  to  $900^\circ\text{C}$ .

### 3.2.3. Temperature programmed oxidation (TPO)

About 70 mg of sample was placed into a porous basket in a Setaram TG85 thermo-balance and heated in air ( $SV = 2 \times 10^{-2} \text{ m}^3 \cdot \text{s}^{-1} \cdot \text{kg}^{-1}$ ) at a heating rate of  $10 \text{ K} \cdot \text{min}^{-1}$  to  $800^\circ\text{C}$ . The carbon content of the sample was calculated from the weight loss between  $300^\circ\text{C}$  and  $800^\circ\text{C}$ . After cooling down to room temperature the colour of all samples was white, indicating complete burn off of carbon.

## 3.3. Dielectric heating

### 3.3.1. Temperature measurement

During drying of the sample in a conventional furnace the temperature of the sample bed was monitored simultaneously with a thermocouple (type K) and an optical fiber. This allows calibration of the optical fiber. A linear correlation was observed between the temperature measured by the thermocouple and the optical fiber.

The temperature in the sample during experiments in the microwave furnace was only measured using an optical fiber. The temperature measurement using optical fibers is restricted to  $>100^\circ\text{C}$ .

### 3.3.2. Microwave set-up

The microwave system (Fig. 1) consists of a microwave source (2450 MHz, 1 kW), a circulator to prevent damage of the microwave source due to reflected microwaves, a 3-stub tuner section, the monomode microwave cavity TE<sub>10</sub> and a water load. Reflection of the microwaves was minimised using the stub tuners. The waveguide is formed by a copper rectangular channel with the dimensions 8.65 cm (width) × 4.375 cm (height). The microwave set-up was operated in travelling wave mode; any microwave energy not absorbed

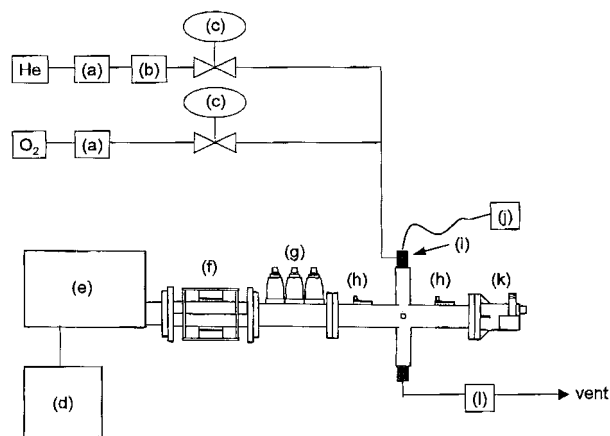


Figure 1 Schematic drawing of 2.45 GHz microwave setup: (a) water trap, (b) oxygen trap, (c) mass flow controller, (d) generator (Muegge, MW-GIR 2 M 167-850-04), (e) microwave source (Muegge, MW-46029-850-01), (f) circulator (Philips, 2722 163 02071), (g) stub tuners (Muegge, MW-7614-0060), (h) power sensor (Rhode & Schwarz, 828.3818.02), (i) quartz tubular reactor, (j) optical fiber (Luxtron, accufiber—OFT lightpipe, straight end), (k) waterload, (l) quadrupole mass spectrometer (Balzers, Prisma QMS 2000).

after passing through the microwave cavity was absorbed by a water load.

A quartz tubular reactor (internal diameter = 18 mm), designed to accommodate an optical fiber, is positioned perpendicular to the direction of propagation. It is filled with a pre-set volume of sample. All samples were crushed and sieved to a particle size of  $\leq 200 \mu\text{m}$ . Throughout all experiments the volume of sample was kept constant ( $10 \text{ cm}^3$ ). Using a conventional furnace the carbonised sample was dried in a He flow ( $GHSV = 6 \times 10^2 \text{ hr}^{-1}$ ) at  $150^\circ\text{C}$  for 1 hour; the heating rate employed was  $5^\circ\text{C}$  per minute. After cooling down to room temperature the sample was transferred to the microwave cavity under a He flow.

The temperature of the sample during dielectric heating was controlled through a temperature control loop coupled to the microwave power and the optical fiber inserted in the sample bed.

## 4. Results and discussion

Several low loss oxidic materials were impregnated with carbon. After polymerisation and carbonisation, dielectric heating experiments of the materials thus obtained were carried out. The resistance of the carbon layer towards oxidation in an oxidising atmosphere during dielectric heating in air was also studied.

### 4.1. Impregnation of low loss oxidic materials with carbon

#### 4.1.1. Polymerisation and carbonisation

Following the impregnation of samples with furfuryl alcohol and polymerisation, a TPD analysis was performed (Fig. 2). After TPD all samples were coloured

TABLE IV Characterisation of the pure oxides

Oxide	Supplier	Name	$S_{\text{BET}}$ (m <sup>2</sup> · g <sup>-1</sup> )	Pore volume (cm <sup>3</sup> · g <sup>-1</sup> )	Pore width (nm)	Density (g · cm <sup>-3</sup> )
$\gamma\text{-Al}_2\text{O}_3$	Ketjen	Ketjen CK300	208	0.5	8.4	3.1
SiO <sub>2</sub>	Grace	Grace 113	325	1.0	10	2.2

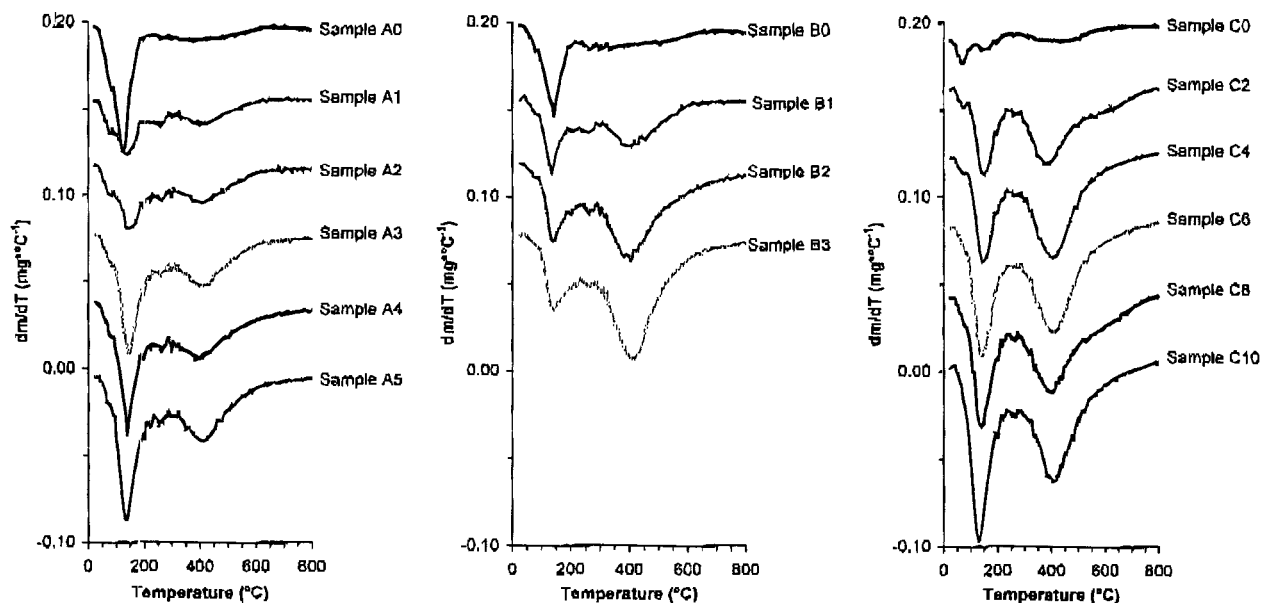


Figure 2 Weight loss as a function of temperature during TPD analysis under an Ar flow of oxides impregnated with polymer of furfuryl alcohol (as indicated in Table I) during various stages of polymerisation. Cylinder shaped  $\gamma$ -Al<sub>2</sub>O<sub>3</sub> extrudates (sample series A, left),  $\gamma$ -Al<sub>2</sub>O<sub>3</sub> sieve fraction (sample series B, middle), SiO<sub>2</sub> (sample series C, right).

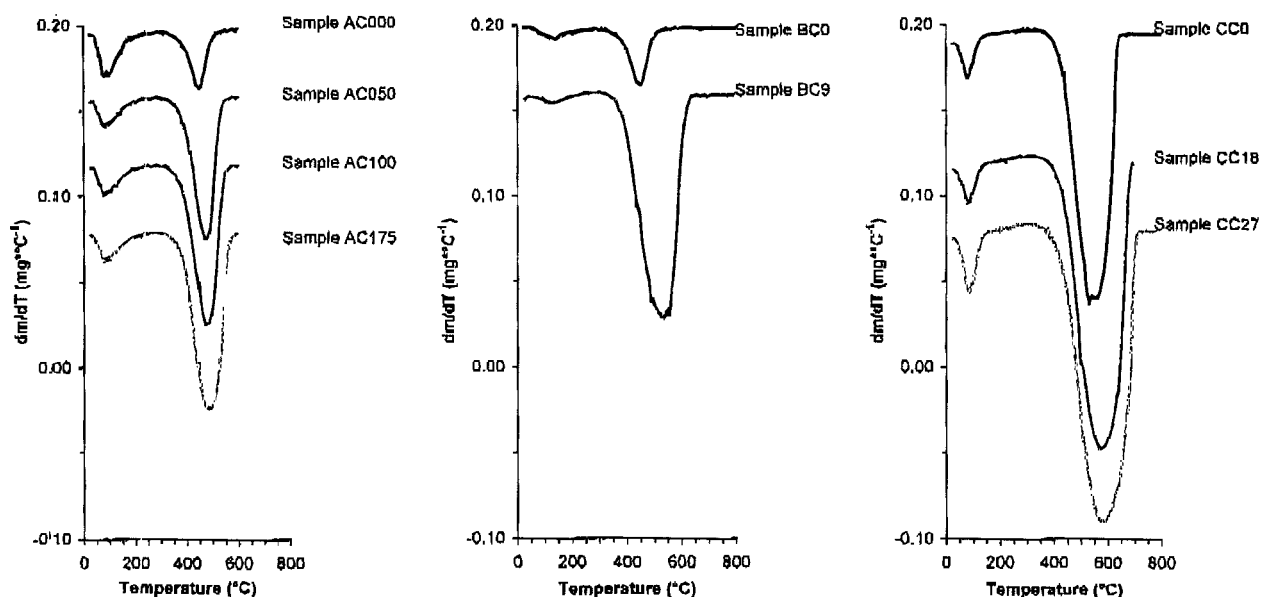


Figure 3 Weight loss as a function of temperature during TPO of samples after carbonisation. Cylinder shaped  $\gamma$ -Al<sub>2</sub>O<sub>3</sub> extrudates (sample series AC, left),  $\gamma$ -Al<sub>2</sub>O<sub>3</sub> sieve fraction (sample series BC, middle), SiO<sub>2</sub> (sample series CC, right).

black. In the TPD patterns the loss of water and furfuryl alcohol is seen between 80°C and 180°C. The region between 300°C and 700°C, with a maximum around 400°C–450°C, corresponds to the carbonisation of the polymer [38].

For all samples one may observe an increasing loss of water during TPD (bands from 80°C to 180°C) with an increasing amount of HNO<sub>3</sub> added during polymerisation. This is due to a higher degree of polymerisation and the thus increased polymer content of the samples. Water formed during polymerisation adsorbs to the oxide and is released only at higher temperatures.

The weight loss during carbonisation in the temperature range 300°C–700°C increases with amount of HNO<sub>3</sub> added during the polymerisation step. Again, this is due to a higher polymerisation rate and conversion.

For further experiments a carbonisation temperature of 550°C was chosen. This is beyond the temperature where maximum in carbonisation rate was observed (400–450°C), but low enough to prevent any sintering of the oxide.

After polymerisation samples were carbonised at 550°C in Ar and subsequently allowed to cool down to room temperature (Table II).

#### 4.1.2. Carbon content

In order to assess the carbon content after carbonisation, carbonised samples were heated in air (Fig. 3).

In the TPO analysis of the carbonised samples (Fig. 3) two regions can be distinguished. At low temperature, between 60°C and 120°C, desorption of moisture is observed. The peak as of 350°C reflects oxidation of the carbon deposited on the oxidic material.

TABLE V Carbon content of different low loss oxides after polymerisation and carbonisation and dielectric heating in a He-flow to 800°C

Sample	Carbon content (wt%)	
	After polymerisation and carbonisation	After dielectric heating to 800°C
AC000	3.4	n.d.
AC050	11.4	n.d.
AC100	14.3	n.d.
AC175	25.8	25.9
BC0	4.9	n.d.
BC9	27.0	27.1
CC0	29.7	27.8
CC18	39.7	39.0
CC27	41.4	42.4

n.d. = not determined.

The maximum of this peak for the alumina-based samples (sample series AC and BC) is at lower temperature (500°C) than for the SiO<sub>2</sub> (sample series CC) based materials (550°C). It is also observed from the TPO analysis that the peak maximum of the oxidation of the carbon shifts to higher temperatures for increasing carbon loadings. This may be due to mass transport limitations.

Using TPO the total carbon loading was assessed. In the case when no nitric acid was added during polymerisation the carbon content of the alumina is less than for SiO<sub>2</sub> (Table V). This remains unexplained as silica is the least acidic oxide and would therefore be expected hardly to catalyse the polymerisation reaction. Possibly, differences in pore size play a role.

#### 4.2. Dielectric heating

Samples were heated in a dielectric field at a linear heating rate. To this end, the temperature of the sample was controlled through an optical fiber temperature control

loop coupled to the microwave source. The successful implementation of this control loop is demonstrated by Fig. 4.

After a stabilisation period of 1 hour the temperature was increased to 800°C at a rate of 2°C · min<sup>-1</sup> and maintained there for an hour.

The optical fiber system used does not allow measurement of temperatures below 100°C. A small overshoot in temperature of approximately 30°C is usually observed at the beginning of the heating process. Therefore no data below 130°C are available.

##### 4.2.1. Heating in an inert gas

After drying the carbonised materials at 150°C in a conventional furnace the samples were heated in the dielectric field in helium to 800°C at a rate of 2°C · min<sup>-1</sup> (Fig. 5).

The absorbed microwave power increases quite sharply with temperature, indicating an increase of the dielectric loss factor. Samples without carbon (not shown) show hardly any microwave absorption and heating of these samples with the power input used beyond 100°C was not observed.

Between 400°C and 500°C an increase in power absorbed is observed. Analysis of the gas flow shows a small release of CO in this temperature range. The carbon content of the samples after dielectric heating is comparable to that before heating (Table V).

After drying in a conventional furnace sample CC27 was first heated in a dielectric field to 600°C. Following cooling to room temperature, the sample was again heated in a dielectric field, now to 800°C. During the first cycle of the repeated heating experiments irreversible changes in the dielectric properties were observed around 500°C (Fig. 6). Subsequent heating of the same sample does not lead to further changes.

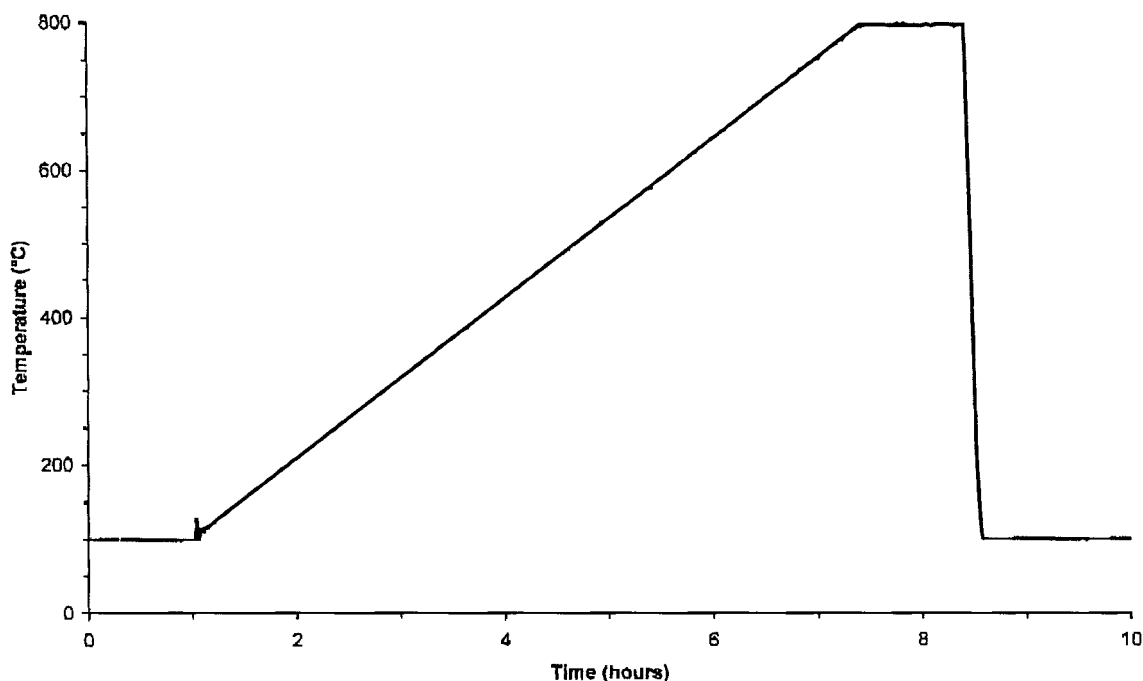


Figure 4 Temperature versus time during dielectric heating (2°C · min<sup>-1</sup>) under a He flow (GHSV = 6 × 10<sup>2</sup> hr<sup>-1</sup>) of cylinder shaped  $\gamma$ -Al<sub>2</sub>O<sub>3</sub> extrudates (sample AC175) after carbonisation and drying.

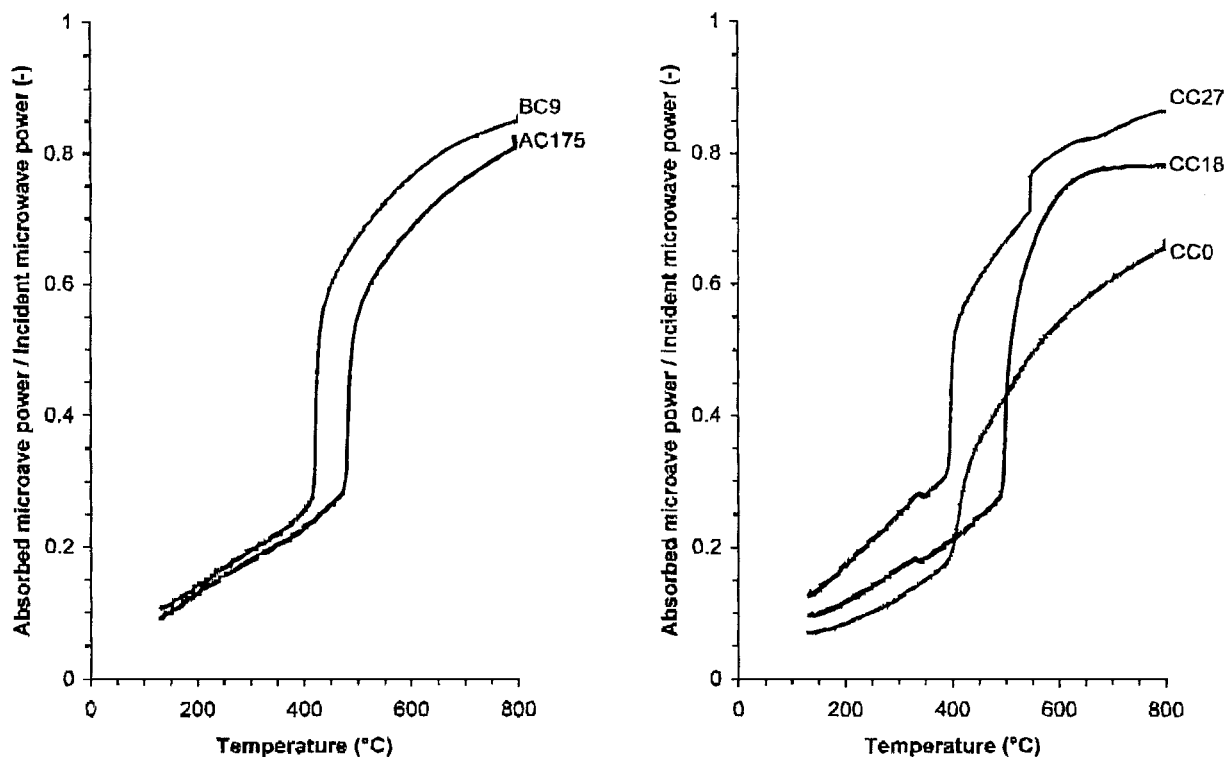


Figure 5 Absorbed microwave power as a function of temperature during dielectric heating ( $2^{\circ}\text{C} \cdot \text{min}^{-1}$ ) under a He flow ( $\text{GHSV} = 6 \times 10^2 \text{ hr}^{-1}$ ) of samples after carbonisation and drying (as indicated in Table II). Cylinder shaped  $\gamma\text{-Al}_2\text{O}_3$  extrudates (sample series AC),  $\gamma\text{-Al}_2\text{O}_3$  sieve fraction (sample series BC),  $\text{SiO}_2$  (sample series CC).

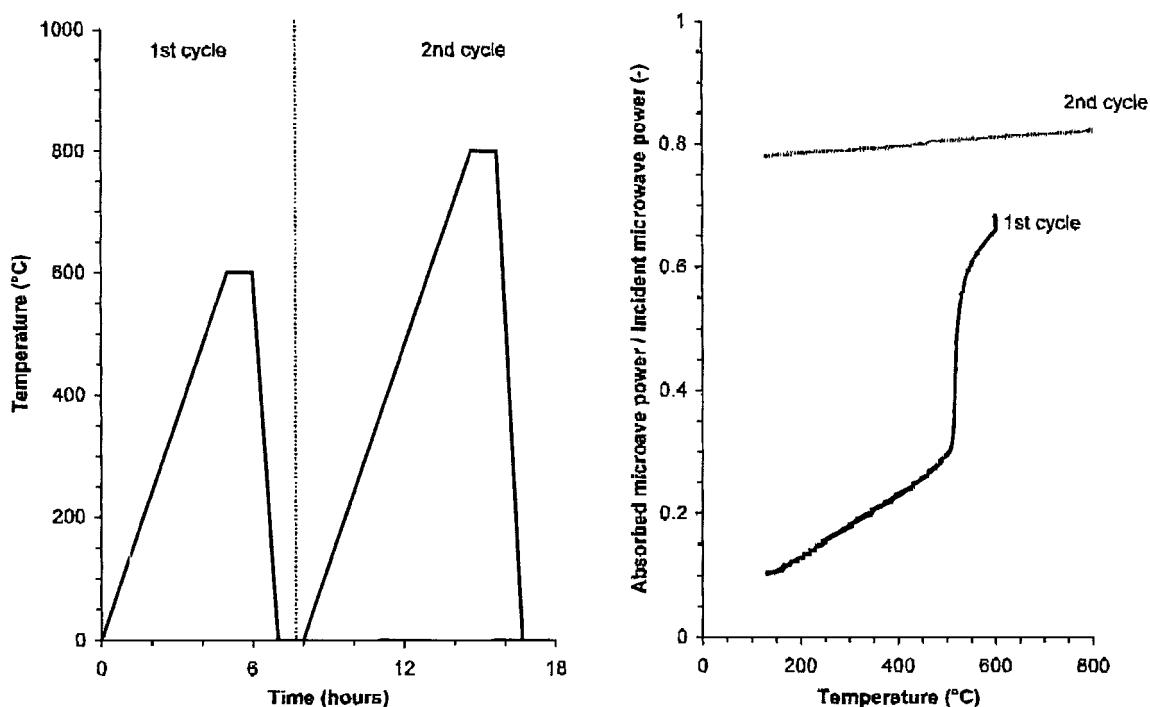


Figure 6 Dielectric heating ( $2^{\circ}\text{C} \cdot \text{min}^{-1}$ ) under a He flow ( $\text{GHSV} = 6 \times 10^2 \text{ hr}^{-1}$ ) of sample CC27 (44wt% C/ $\text{SiO}_2$ ) after carbonisation and drying. The sample was first heated to  $600^{\circ}\text{C}$  (1st cycle). After allowing to cool down to room temperature the same sample was re-heated to  $800^{\circ}\text{C}$  (2nd cycle). Left: temperature as a function of time; right: absorbed microwave power as a function of temperature.

Norit RX3 Extra is a non-graphitisable carbon with a surface covered by chemisorbed oxygen [41]. In a microwave field the carbon is readily heated to  $800^{\circ}\text{C}$  in a He flow (Fig. 7). The dielectric loss factor is constant up to  $800^{\circ}\text{C}$ . Therefore the observed change in structure during dielectric heating of the carbon coated low loss oxides cannot be attributed to the reaction of chemisorbed oxygen with the carbon.

Reaction of the carbon with the oxide, thereby forming carbides, is unlikely as this kind of process proceeds at temperatures around  $1600^{\circ}\text{C}$  [10, 11, 42].

The observed sudden increase of the dielectric loss factor indicates some kind of change in structure of the samples. As all samples tested show this behaviour it is reasonable to suspect that the carbon coating of the samples undergoes a change in structure, whereby

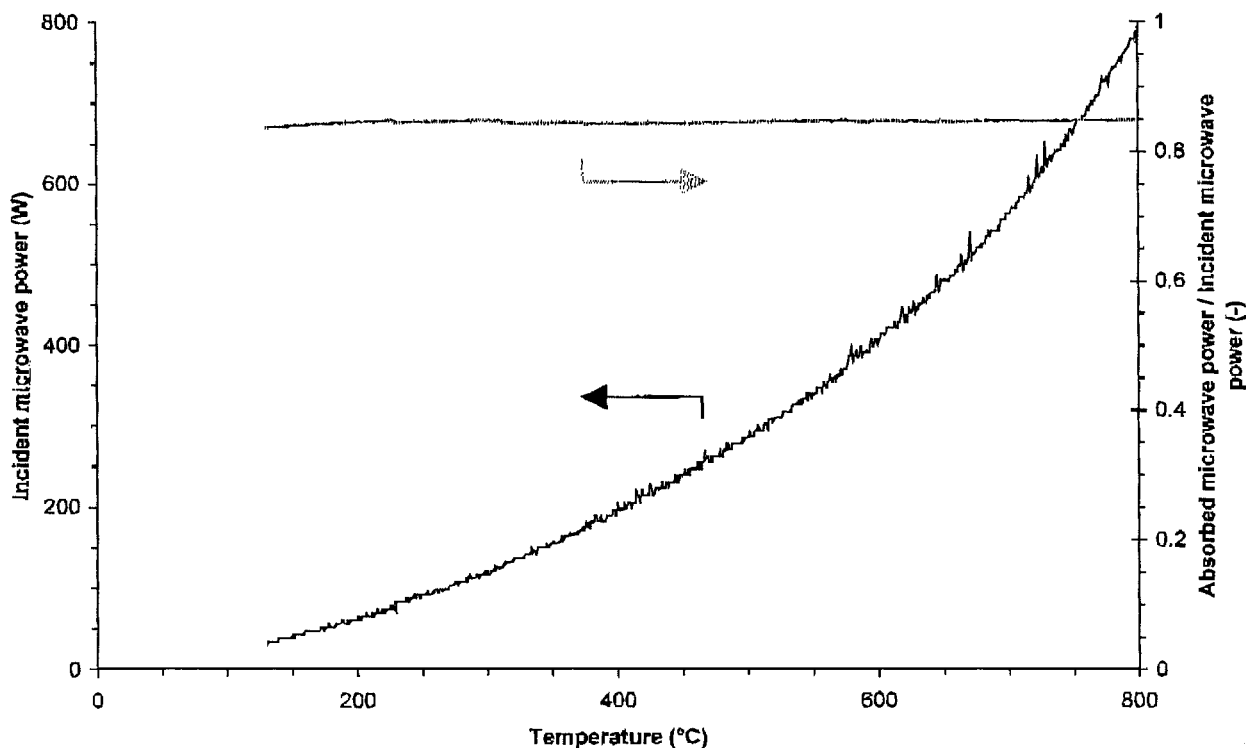


Figure 7 Dielectric heating ( $2^{\circ}\text{C} \cdot \text{min}^{-1}$ ) under a He flow ( $\text{GHSV} = 6 \times 10^2 \text{ hr}^{-1}$ ) of Norit RX3 extra after drying at  $150^{\circ}\text{C}$  in a conventional furnace. Incident microwave power and absorbed microwave power as a function of temperature.

the dielectric loss factor of the material increases. At  $800^{\circ}\text{C}$  the dielectric loss factor of the low loss oxide impregnated samples is comparable to that of Norit RX3 Extra (Figs 5 and 7 respectively). In view of the density differences between the materials this is not surprising.

From the experiments it is clear that the dielectric loss factor of the samples is enhanced significantly by the presence of the carbon coating. A plot of the dielectric loss factor as a function of the volume fraction of carbon in the samples (Equation 2) shows that the dielectric loss factor is proportional to the carbon content (Fig. 8). It would therefore be expected that the absorbed microwave power increases with carbon content. The samples were heated to  $800^{\circ}\text{C}$  at a rate of  $2^{\circ}\text{C} \cdot \text{min}^{-1}$  under a He flow and kept at  $800^{\circ}\text{C}$  for an hour, so that steady state conditions were achieved. The fraction of microwave power absorbed at  $800^{\circ}\text{C}$  as a function of the amount of carbon present in the reactor is also shown in Fig. 8.

The complex permittivity of some porous ceramics and carbonaceous materials are shown in Table VI. Unfortunately the temperature at which the dielectric properties were measured are not always clearly mentioned.

The dielectric loss factor of sample series CC (samples based on  $\text{SiO}_2$ ), e.g., the absorbed microwave power, is proportional to the carbon content of the samples [13]. The samples based on  $\text{Al}_2\text{O}_3$  (samples series AC and BC), however, deviate from this trend. Apparently an effect of the support material exists that influences the dielectric loss factor. At high temperature it may be possible that the  $\epsilon''$  of  $\text{Al}_2\text{O}_3$  or  $\text{SiO}_2$  approach that of carbon.

The theoretical dielectric loss factor based on the Rayleigh equation is in qualitative agreement with the measured absorbed microwave power, e.g., the dielectric loss factor increases with carbon content. At room

TABLE VI Complex permittivity of porous oxide ceramics and carbonaceous materials at 2.45 GHz

Material	$\epsilon'$ (-)	$\epsilon''$ (-)	Temperature ( $^{\circ}\text{C}$ )	Ref.
$\alpha$ - $\text{Al}_2\text{O}_3$	8–10	0–1	100–1200	[44]
$\gamma$ - $\text{Al}_2\text{O}_3$	3.006	0.1720	Room temperature <sup>a</sup>	[13]
$\text{SiO}_2$	3.066	0.215	Room temperature <sup>a</sup>	[13]
Active carbon	7	2	Room temperature <sup>a</sup>	[45]
Soot	$\sim 10$	$\sim 3$	Room temperature <sup>a</sup>	[13]

<sup>a</sup>Temperature at which dielectric properties were measured not clearly mentioned by the authors.

temperature the Rayleigh mixture equation predicts a dielectric loss factor which is proportional to the total carbon volume fraction, on account of the comparatively high value of  $\epsilon''$  for carbon. Extrapolation of the Rayleigh equation to higher temperatures is tempered by the lack of  $\epsilon''$  data at high temperature. It is known that dielectric properties are temperature dependent (see for instance the data on  $\alpha$ - $\text{Al}_2\text{O}_3$  in Table VI). Also, the Rayleigh mixture equation is only valid for isolated, conducting particles suspended in a non-conducting medium.

#### 4.2.2. Heating in an oxygen-containing atmosphere

After drying the carbonised materials at  $150^{\circ}\text{C}$  in a conventional furnace samples were tested for dielectric heating in  $\text{O}_2/\text{He}$  (0.5vol%  $\text{O}_2$ ,  $\text{GHSV} = 6 \times 10^2 \text{ hr}^{-1}$ ) to a set-point of  $800^{\circ}\text{C}$  at a rate of  $2^{\circ}\text{C} \cdot \text{min}^{-1}$  (Fig. 9).

The absorbed microwave power, e.g., the dielectric loss factor, while heating in He is comparable for the  $\text{Al}_2\text{O}_3$  based sample (sample BC9) and the  $\text{SiO}_2$  based sample (sample CC27). Initially the dielectric loss factor increases with temperature. However, due to the oxygen atmosphere the carbon is oxidised at

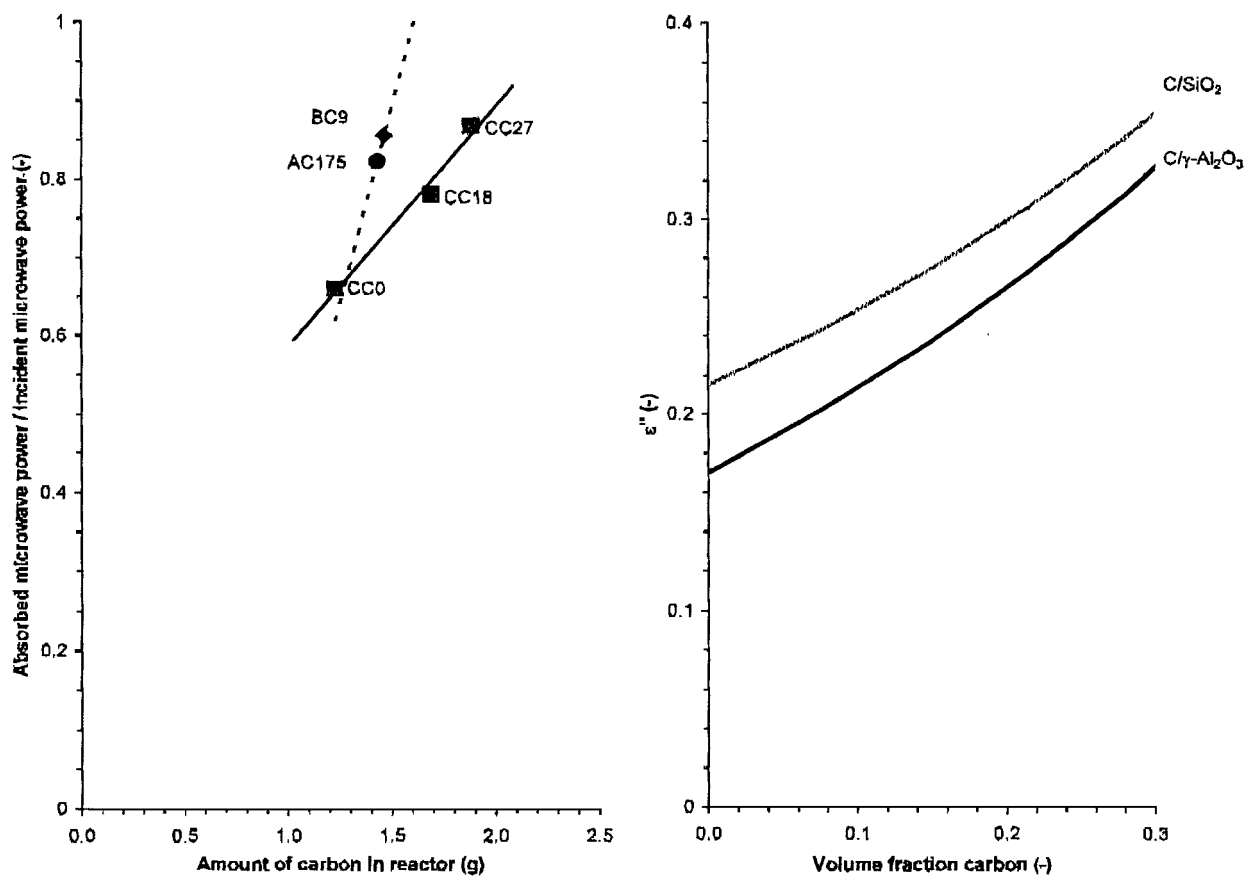


Figure 8 Left: Absorbed microwave power as a function of carbon content of samples after carbonisation and drying. Data shown are under steady state conditions at 800°C. (●) Cylinder shaped  $\gamma$ -Al<sub>2</sub>O<sub>3</sub> extrudates (sample series AC), (◆)  $\gamma$ -Al<sub>2</sub>O<sub>3</sub> sieve fraction (sample series BC), (■) SiO<sub>2</sub> (sample series CC). Right: modeling of dielectric loss factor,  $\epsilon''$ , at room temperature as a function of carbon content using the Rayleigh mixture equation (density of  $\gamma$ -Al<sub>2</sub>O<sub>3</sub> and SiO<sub>2</sub> in Table IV; density of amorphous carbon taken as 2000 kg · m<sup>-3</sup> [43];  $\epsilon''$  of  $\gamma$ -Al<sub>2</sub>O<sub>3</sub>, SiO<sub>2</sub> and activated carbon in Table VI).

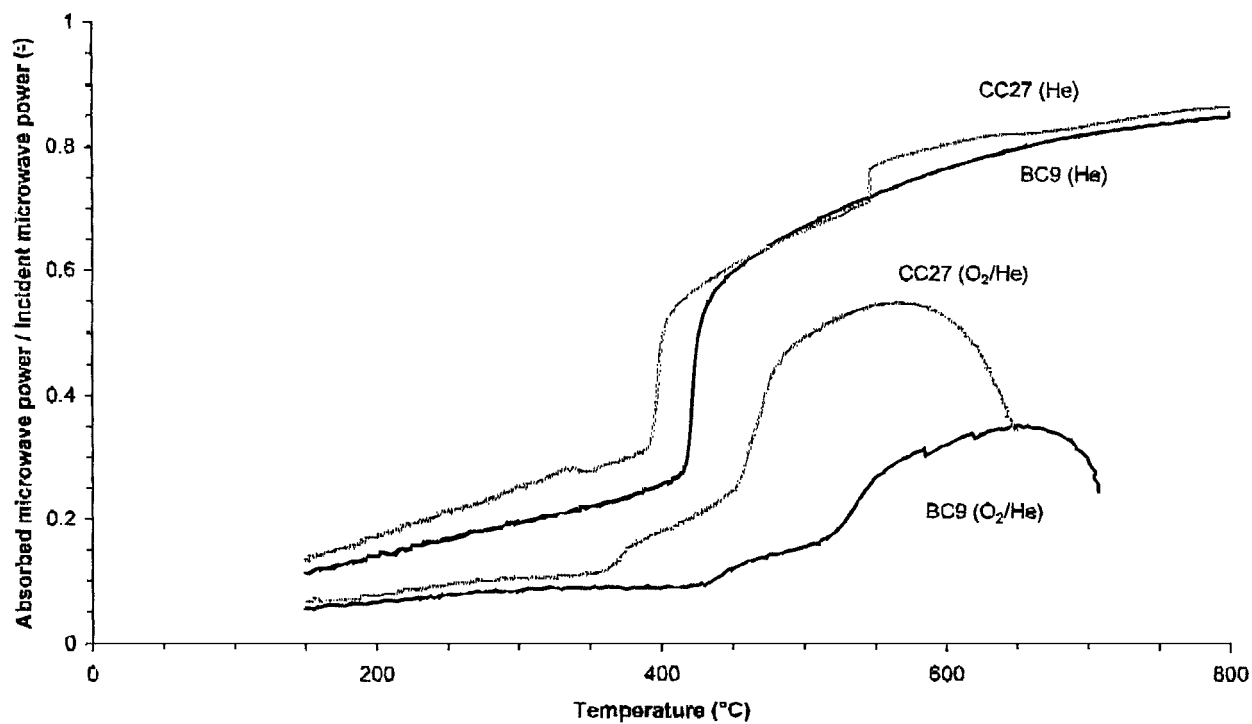


Figure 9 Absorbed microwave power as a function of temperature during dielectric heating (2°C · min<sup>-1</sup>) under a He flow or O<sub>2</sub>/He flow (0.5 vol% O<sub>2</sub>) (GHSV = 6 × 10<sup>2</sup> hr<sup>-1</sup>) of samples after carbonisation and drying,  $\gamma$ -Al<sub>2</sub>O<sub>3</sub> sieve fraction (sample BC9), and SiO<sub>2</sub> (sample CC27).

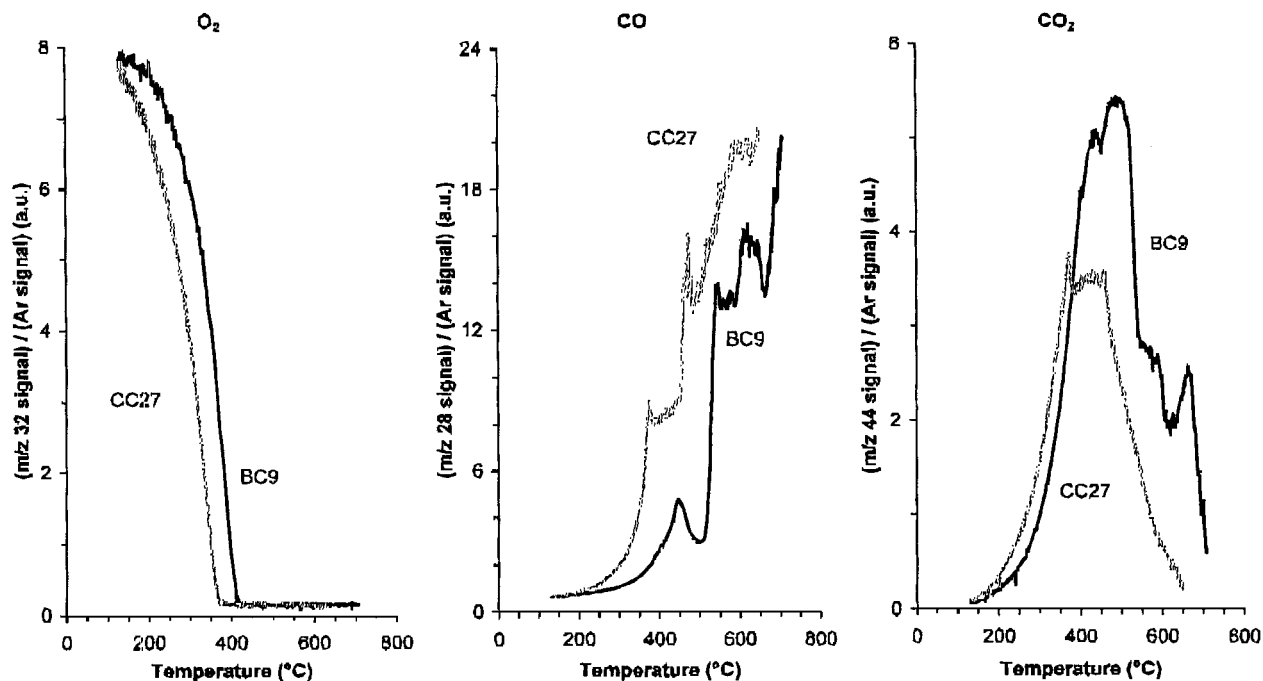


Figure 10 Analysis of gas phase composition during dielectric heating with a linear heating rate ( $2^{\circ}\text{C}\cdot\text{min}^{-1}$ ) under a  $\text{O}_2/\text{He}$  flow (0.5 vol%  $\text{O}_2$ , GHSV =  $6 \times 10^2 \text{ hr}^{-1}$ ) of samples after carbonisation and drying.  $\gamma\text{-Al}_2\text{O}_3$  sieve fraction (sample BC9),  $\text{SiO}_2$  (sample CC27). Three masses were monitored as a function of temperature:  $\text{O}_2$  (left),  $\text{CO}$  (middle), and  $\text{CO}_2$  (right).

temperature beyond  $400^{\circ}\text{C}$  and concurrently the dielectric loss factor is reduced. As a consequence the final temperatures reached in helium are no longer obtained.

For all samples the oxygen consumption starts around  $150^{\circ}\text{C}$  (Fig. 10). The conversion of oxygen reaches 100%. The rate at which the oxygen is consumed, e.g., the combustion rate, increases in the series  $\text{BC9} < \text{CC27}$ . It was also observed that the temperature at which the dielectric loss factor reaches a maximum increases in the series  $\text{CC27} < \text{BC9}$ . The rate at which the carbon is combusted clearly differs between the samples.

The carbon is oxidised to  $\text{CO}$  and  $\text{CO}_2$ .  $\text{CO}_2$  production reaches a maximum between  $300^{\circ}\text{C}$  and  $500^{\circ}\text{C}$ , whereas  $\text{CO}$  is mainly observed between  $500^{\circ}\text{C}$  and  $700^{\circ}\text{C}$ . Below  $500^{\circ}\text{C}$ , oxygen absorbs onto the carbon surface forming absorbed  $\text{CO}$  species. These species further react with oxygen to  $\text{CO}_2$ . At higher temperatures,  $\text{CO}_2$  reacts with the carbon to  $\text{CO}$ .

## 5. Conclusions

Oxides, such as alumina and silica, do not heat up well in a dielectric field due to the low dielectric loss factor. This loss factor can be enhanced significantly by impregnation of these oxides with amorphous carbons, being a suitable microwave susceptor material. In this way heating of alumina and silica the material in a dielectric field up to at least  $800^{\circ}\text{C}$  is possible.

A suitable way to impregnate porous oxides is by impregnation and subsequent polymerisation of furfuryl alcohol, followed by carbonisation at  $550^{\circ}\text{C}$  of the polymer. The ultimate carbon content obtained can easily be controlled during the polymerisation through the amount of acid used as the polymerisation catalyst.

The dielectric loss factor of carbon-impregnated low loss oxides increases with temperature and is roughly

proportional to the carbon content in accordance with the Rayleigh mixture equation. Under He, an irreversible and as yet unexplained change in the impregnated carbon is observed between  $400^{\circ}\text{C}$  and  $500^{\circ}\text{C}$ , with a concurrent increase in the dielectric loss factor.

Carbon impregnation may be utilised to allow it to be temporarily heated in a dielectric field under a flow of air or oxygen. Beyond  $350^{\circ}\text{C}$  this carbon starts to be oxidised, producing additional heat to heat up the sample. Maximum temperatures reached are less than for dielectric heating in inert gas. This principle could be used in curing of low loss ceramics.

## Acknowledgements

The Graduate School for Process Technology OSPT is gratefully acknowledged for financial support.

## References

1. N. G. EVANS, M. G. HAMYLN and A. L. BOWDEN, *British Ceramic Transactions* **95** (1996) 62.
2. M. WILLERT-PORADA, *Mat. Res. Soc. Symp. Proc.* **347** (1994) 31.
3. Z. XIE, J. YANG, X. HUANG and Y. HUANG, *Journal of the European Ceramic Society* **19** (1999) 381.
4. G. J. VOGT and W. P. UNRUH, *Ceram. Trans.* **36** (1993) 297.
5. Y. XU and X. XIAO, *J. Mater. Res.* **10** (1995) 334.
6. K. J. RAO, B. VAIDHYANATHAN, M. GANGULI and P. A. RAMAKRISHNAN, *Chem. Mater.* **11** (1999) 882.
7. S. ANANTHAKUMAR, U. S. HAREESH, A. D. DAMODARAN and K. G. K. WARRIER, *British Ceramic Transactions* **97** (1998) 236.
8. *Idem.*, *J. Mater. Sci. Lett.* **17** (1998) 145.
9. R. MOENE, PhD thesis, Delft University of Technology, Delft (1995).
10. L. CEROVIC, S. K. MILONJIC and S. P. ZEC, *Ceram. Int.* **21** (1995) 271.
11. A. AMROUNE, G. FANTOZZI, J. DUBOIS, J. P. DELOUME, B. DURAND and R. HALIMI, *Mater. Sci. Eng. A: Struct. Mater.* **290** (2000) 11.

12. C. P. LORENSEN, M. C. L. PATTERSON, G. RISTO and R. KIMBER, *Mat. Res. Soc. Symp. Proc.* **269** (1992) 129.
13. J. MA, M. FANG, P. LI, B. ZHU, X. LU and N. T. LAU, *Appl. Catal. A: General* **159** (1997) 211.
14. S. L. MCGILL and J. W. WALKIEWICZ, *J. Microwave Power Electromag. Energy Symp.* **22** (1987) 175.
15. J. W. WALKIEWICZ, G. KAZONICH and S. L. MCGILL, *Minerals and Metallurgical Processing* **5** (1988) 39.
16. N. STANDISH and W. HUANG, *ISIJ International* **31** (1991) 241.
17. S. MARLAND, B. HAN, A. MERCHANT and N. ROWSON, *Fuel* **79** (2000) 1283.
18. N. A. ROWSON and N. M. RICE, *Minerals Engineering* **3** (1990) 363.
19. S. BODMAN, P. MONSEF-MIRZAI, H. MANAK and W. R. McWHINNIE, *Fuel* **76** (1997) 1315.
20. J. T. STRACK, I. S. BALBAA and B. T. BARBER, *Ceram. Trans.* **59** (1995) 99.
21. S. M. BRADSHAW, E. J. VAN WYK and J. R. DE SWARDT, *The Journal of The South African Institute of Mining and Metallurgy* July/August (1998) 201.
22. J. A. MENÉNDEZ, E. M. MENÉNDEZ, A. GARCÍA, J. B. PARRA and J. J. PIS, *J. Microwave Power Electromag. Energy* **34** (1999) 137.
23. L. M. NORMAN and C. Y. CHA, *Chemical Engineering Communications* **140** (1996) 87.
24. C.-Y. CHA and B. I. KIM, *Fuel Sci. Tech. Intl.* **11** (1993) 1175.
25. P. MONSEF-MIRZAI, M. RAVINDRAN, W. R. McWHINNIE and P. BURCHILL, *Fuel* **74** (1995) 20.
26. M. Y. TSE, M. C. DEPEW and J. K. S. WAN, *Res. Chem. Intermed.* **13** (1990) 221.
27. M. S. IOFFE, S. D. POLLINGTON and J. K. S. WAN, *J. Catal.* **151** (1995) 349.
28. M. EL MALHI, M. E. ACHOUR, F. LAHJOMRI and Y. BENSALAH, *J. Mater. Sci. Lett.* **18** (1999) 613.
29. M. E. ACHOUR, M. EL MALHI, J. L. MIANE, F. CARMONA and F. LAHJOMRI, *J. Appl. Poly. Sci.* **73** (1999) 969.
30. J. P. R. VISSERS, F. P. M. MERCX, S. M. A. M. BOUWENS, V. H. J. DE BEER and R. PRINS, *J. Catal.* **114** (1988) 291.
31. J. A. ALCAÑIZ-MONGE, D. CAZORLA-AMORÓS, A. LINARES-SOLANO, E. MORALLÓN and J. L. VÁZQUEZ, *Carbon* **36** (1998) 1003.
32. E. M. DELISO, K. P. GADKAREE, J. F. MACH and K. P. STREICHER, US Patent, 5,451,444 (1995).
33. *Idem.*, US Patent, 5,597,617 (1997).
34. K. P. GADKAREE, US Patent, 5,487,917 (1996).
35. *Idem.*, *Carbon* **36** (1998) 981.
36. X. XU and J. A. MOULIJN, *Chem. Ind.* **71** (1998) 599.
37. E. E. HUCKE, US Patent, 3,859,421 (1975).
38. T. VERGUNST, F. KAPTEIJN and J. A. MOULIJN, *Stud. Surf. Sci. Catal.* **118** (1998) 175.
39. G. ROUSSY and J. A. PEARCE, in "Foundations and Industrial Applications of Microwaves and Radio Frequency Fields" (John Wiley & Sons Ltd, Chichester, 1995).
40. S. NELSON, A. KRASZEWSKI and T. YOU, *J. Microwave Power Electromag. Energy* **26** (1991) 45.
41. H. MARSH, in "Structure in Carbons," edited by J. L. Figueiredo and J. A. Moulijn (Martinus Nijhof Publishers, Dordrecht, 1986).
42. M. NARISAWA, K. YAMANE, Y. OKABE, K. OKAMURA and Y. KURACHI, *J. Mater. Res.* **14** (1999) 4587.
43. D. R. LIDE and H. P. R. FREDERIKSE, in "CRC Handbook of Chemistry and Physics" (CRC Press, New York, 1998).
44. J. G. P. BINNER, J. A. FERNIE, P. A. WHITAKER and T. E. CROSS, *J. Mater. Sci.* **33** (1998) 3017.
45. M. AKHOUAOU, B. SRHIR, H. AMMOR, K. CHLIHI, M. HABIBI and M. EL KADIRI, *Environ. Technol.* **21** (2000) 681.

*Received 30 October 2000  
and accepted 20 June 2002*